Virologica Sinica 37 (2022) 740–745

Contents lists available at ScienceDirect

Virologica Sinica

journal homepage: www.keaipublishing.com/en/journals/virologica-sinica
www.virosin.org

Research Article

The infectivity and pathogenicity of hepatitis A virus live-attenuated vaccine strain H2 in type I interferon receptor-deficient mice

Qing-Qing Ma [a,1], Hong-Jiang Wang [b,1], Jian Li [a,c], Meng-Qi Li [a], Tian-Shu Cao [a], Xiao-Yan Wu [a], Hong-Ying Qiu [a], Hui Zhao [a,*], Cheng-Feng Qin [a,d,*]

[a] State Key Laboratory of Pathogen and Biosecurity, Beijing Institute of Microbiology and Epidemiology, Academy of Military Medical Sciences (AMMS), Beijing, 100071, China
[b] Department of Comprehensive Basic Experiment, The Chinese People's Liberation Army Strategic Support Force Characteristic Medical Center, Beijing, 10010, China
[c] School of Medicine, Tsinghua University, Beijing, 100084, China
[d] Research Unit of Discovery and Tracing of Natural Focus Diseases, Chinese Academy of Medical Sciences, Beijing, 650018, China

ARTICLE INFO

Keywords:
Hepatitis A virus (HAV)
Hepatitis A
Mouse model
Live-attenuated vaccine

ABSTRACT

Hepatitis A virus (HAV) live-attenuated vaccine H2 strain has been approved for clinical use for decades with ideal safety profiles in nonhuman primate models and humans. Recently, type I interferon (IFN) receptor-deficient mice were shown to be susceptible to HAV infection. Herein, we sought to determine the infection and replication dynamics of the H2 in *Ifnar*$^{-/-}$ mice that lack type I IFN receptor. Following intravenous injection, the H2 failed to cause obvious clinical symptoms in *Ifnar*$^{-/-}$ mice, and no significant upregulation in serum alanine aminotransferase (ALT) levels was observed. Notably, the histopathological examination showed that there were significant focal infiltrations of lymphocytes and neutrophils in the portal area, but no focal necrosis was observed in liver tissues. Viral RNAs sustained in the liver, and the infectious virus could be recovered from the liver tissue until 42 days post-infection. More importantly, H2 infection induced obvious viremia and persistent viral shedding in feces. In addition, robust HAV-specific humoral immune responses were induced in *Ifnar*$^{-/-}$ mice. Overall, our study revealed the safety profile of H2 in *Ifnar*$^{-/-}$ mice, which not only helps understand the attenuation mechanism of H2, but also expands the application of the *Ifnar*$^{-/-}$ mouse model for HAV studies.

1. Introduction

Hepatitis A is a major public health threat worldwide and frequently occurs in developing countries (Bamford and Zuckerman, 2021). According to a new estimation by WHO, 100 million hepatitis A infections and 1.5 million symptomatic cases were reported annually worldwide and are responsible for 15,000 to 30,000 deaths per year (Daniel and Pierre, 2019). Hepatitis A is a self-limited hepatitis that usually resolves without permanent sequelae within 4–7 weeks. However, severe fulminant hepatitis with potentially lethal liver failure can occur, particularly in older individuals (Guidotti et al., 2019). Symptoms of hepatitis A include fatigue, nausea, stomach pain, and jaundice, and can last up to two months (Hirai-Yuki et al., 2016b). In recent years, an expansion of infection has been of great concern in Europe and America (Yin et al., 2020; Oluwafemi et al., 2022).

Hepatitis A is caused by Hepatitis A virus (HAV) infection. HAV is a single-stranded, positive-sense RNA virus with a 7.5 kb genome consisting of a open reading frame (ORF) flanked by a 5′-untranslated region (UTR) and 3′-UTR. The ORF encodes a single large polyprotein that is processed into four structural proteins (VP4, VP2, VP3, and VP1pX) and six non-structural proteins (2B, 2C, 3A, 3B, 3C, and 3D) (Drexler et al., 2015). The best way to prevent hepatitis A infection is through vaccination. Currently, two types of hepatitis A vaccines are used worldwide. Formaldehyde-inactivated hepatitis A virus (HAV) vaccines are used in most countries (Luo et al., 2019). The live attenuated hepatitis A vaccine produced from HAV H2 strain is in routine use in China since 1992, and included in Expanded Program on Immunization (EPI) since 2007 (Zhuang et al., 2012). The live attenuated hepatitis A vaccine has shown high immunogenic and long-term protection efficacy in the vaccinated population (Rao et al., 2016; Shah et al., 2020).

* Corresponding authors.
E-mail addresses: shuishu2002@126.com (H. Zhao), qincf@bmi.ac.cn (C.-F. Qin).
[1] Qing-Qing Ma and Hong-Jiang Wang contributed equally to this work.

https://doi.org/10.1016/j.virs.2022.07.009
Received 22 April 2022; Accepted 23 May 2022
Available online 19 July 2022

Currently, non-human primates are the only animal model used to evaluate hepatitis A vaccine, because this specie can produce clinical symptoms similar to human HAV infection (Mao et al., 1981; Purcell and Emerson, 2001). Some studies have also reported that guinea pigs can be infected with HAV. However, clinical symptoms and infection characteristics vary greatly among individuals in HAV-infected guinea pigs (Britt et al., 2001). Recently, Lemon and colleagues demonstrated that type I interferon receptor-deficient mice are highly susceptive to HAV, and intravenous injection with wild type strain leads to the serum alanine aminotransferase (ALT) level elevation, hepatocellular apoptosis, and inflammatory responses similar to the symptoms of human liver injury (Hirai-Yuki et al., 2016a).

The live-attenuated HAV vaccine strain H2 was developed through a series of passages in cell cultures and shows evidence of virulence in nonhuman primate models and humans (Mao et al., 1989). However, the infection characteristics of H2 strain in small animal models are still unclear, which hinders the study of the attenuation mechanism of H2. In this study, *Ifnar*$^{-/-}$ mice were employed to clarify the infection and pathogenicity caused by the H2 strain, which helps us further explore the attenuation mechanism of the H2 and expands the application of *Ifnar*$^{-/-}$ mouse model for HAV study.

2. Materials and methods

2.1. Virus and cells

Human fetal lung diploid fibroblastic cells (2BS, ATCC bio-53536), and African green monkey kidney cells (BS–C-1, ATCC CCL-26) were purchased from ATCC. 2BS cells were maintained in MEM Alpha basic (Gibco, USA) supplemented with penicillin (100 U/mL), streptomycin (100 μg/mL), and 10% FBS. BS-C-1 cells were cultured in Dulbecco's Modified Eagle Medium (DMEM, Gibco, USA) supplemented with penicillin (100 U/mL), streptomycin (100 μg/mL), and 10% FBS. The two cells were grown at 37 °C in 5% CO_2.

HAV vaccine strain H2 (GenBank accession no. EF406359) was kindly provided by the Institute of Medical Biology, Chinese Academy of Medical Sciences (Kunming, China). Virus stocks were prepared in 2BS cells and stored in aliquots at −80 °C. Virus titers were determined by standard RT-qPCR as described below. HAV strain HM175/18f (GenBank accession no. M59808) was kindly provided by Prof. Qiang Ding (Tsinghua University, Beijing).

2.2. Quantitative reverse transcription PCR (RT-qPCR)

Viral RNA was extracted from samples using a PureLink RNA mini kit (Thermo Fisher Scientific) according to the manufacturer's procedures. HAV genomic RNA was quantified by One Step PrimeScript RT-PCR Kit (Takara, Japan) with the following primers: 5′- GGTAGGCTACGGGTGAAAC-3′ and 5′-AACAACTCACCAATATCCGC-3′ (Hirai-Yuki et al., 2016b). HAV RNA levels were determined by reference to a standard curve generated with synthetic HAV cDNA targeting the 5′ UTR gene.

2.3. Mouse experiments

Ifnar$^{-/-}$ mice (129Sv/Ev mice deficient in type I IFN receptors) were kindly provided by Qi-Bin Leng (Institute Pasteur of Shanghai, Chinese Academy of Sciences) (Li et al., 2013).

A group of female *Ifnar*$^{-/-}$ mice (6–7 weeks, n = 3) were inoculated with 10^7 RNA copies of H2 in 100 μL, or an equal volume of PBS through the intravenous route (i.v.). All mice were observed daily. Serum and feces were collected on day 7, 14, 21, 28, 35, and 42 post-inoculation for determination of viral RNA, ALT, HAV-specific IgG, and neutralizing antibody levels. Mice were sacrificed, and the liver was collected on day 42 post-infection and used for viral RNA measurement, immunohistochemistry, *in situ* hybridization (ISH), and histopathology assays.

2.4. Alanine aminotransferase assay (ALT)

Serum ALT activity was measured using the alanine transaminase activity assay kit with Color Endpoint (Abcam, USA) according to the manufacturer's procedure. Briefly, serum samples were added to the microplate wells followed by the addition of 100 μL of reaction mix. After 10 min of reaction, the microplate was set on a microplate reader in a kinetic model, and values were measured every 2–3 min for at least 60 min at 37 °C using a Colorimetric assay at OD570nm.

2.5. Histopathology analysis

Ifnar$^{-/-}$ mice infected with H2 were sacrificed on day 42, and the liver was excised and fixed with 4% neutral-buffered formaldehyde for 48 h. After being dehydrated and embedded in paraffin, the liver was sectioned into 4 μm in thickness and stained with hematoxylin and eosin (H&E) according to standard procedures for examination by light microscopy (OLYMPUS, Japan).

2.6. Viral RNA in situ hybridization (ISH)

The RNA ISH assay was performed with RNAscope 2.5 HD Reagent Kit (Advanced Cell Diagnostics, USA) according to the manufacturer's instructions. In brief, fixed tissue on slides was treated with RNAscope® Pretreatment Kit to expose target RNA and HAV-spicific probes was designed for target genes to hybridize with target RNA. HAV-special signal was amplificated by using RNAscope® Detection Kit according to the manufacturer's instructions. Tissues were counterstained with Gill's hematoxylin and visualized with standard bright-field microscopy.

2.7. Immunohistochemistry (IHC)

The paraffin tissue sections were deparaffinized and rehydrated before antigen retrieval. Then, the sections were placed in 3% hydrogen peroxide and incubated at room temperature in darkness for 25 min to blocking endogenous peroxidase activity. After being blocked with 3% BSA at room temperature for 1 h, tissue sections were incubated at room temperature with a mouse anti-HAV monoclonal antibody (1:50, Creative Diagnostics, USA) for 1 h. Tissue sections were then washed three times with PBS and incubated with PBS containing a 1:1000 dilution of goat anti-mouse horseradish peroxidase (HRP) antibody (Abcam, USA) for 1 h at room temperature. Tissue sections were then washed three times, and staining was developed using DAB chromogenic reaction. The nucleus is stained with hematoxylin in blue. The images of IHC staining were obtained by an Olympus microscope (Tokyo, Japan).

2.8. Isolation and sequencing of the virus

2BS cells were inoculated with liver extracts from H2 strain-infected mice, and HAV RNA was detected using RT-qPCR in cell cultures at different time points. The total RNA was extracted from the 2BS cell cultures at day 6 post inoculation using a PureLink RNA mini kit (Thermo Fisher Scientific, USA) according to the manufacturer's instructions. Viral genome cDNA was obtained by RT-PCR using the SuperScript III (Thermo Fisher Scientific, 18080400) and used for PCR amplification. The whole ORF was amplified using Phusion High Fidelity PCR Master Mix and the sequencing primers (Supplementary Table S1), and sent for sequencing by Sangon Biotech (Shanghai) Co., Ltd.

2.9. Enzyme-linked immunosorbent assay

The HAV-specific IgG antibody titers were measured by ELISA (Chengzhi Kewei Biological Technology Co., Ltd., China). First, the ELISA plate (96 well) was pre-coated with HAV VP1 antigen (2 μg/mL, 100 μL each well). Then, 50 μL of serum was added to the plates, followed by the addition of 100 μL of enzyme conjugate. The plates were covered with an

adhesive strip and incubated in the dark for 60 min at 37 °C. Then, 50 μL of substrate A and of substrate B were added to each well. After gently shaking and incubation for 15 min at 37 °C, the plates were added with 50 μL of stop solution. The absorbance at 450 nm was measured and accurate quantification was conducted using SpectraMax iD3 (Molecular Devices).

2.10. Virus neutralization assay

Mice serum was harvested at 42 days post infection and heat inactivated. The serum of infected (H2 group) and uninfected mice (Mock group) was diluted ten times, respectively. Then the ten-fold diluted serum or PBS (NC group) was co-incubated with HM175/18f strain for 1 h at 37 °C, and subsequently, the mixture was used to infect BS-C-1 cells in 12-well plates. After 8 days of infection, the cells were fixed with formaldehyde and stained with neutral red, and the number of plaques was counted.

2.11. Statistical analysis

All statistical analysis were performed with GraphPad Prism software version 8.0 (GraphPad Prism Software Inc., CA, USA), and non-parametric statistical analysis was used to determine statistical significance between two groups ($*P < 0.05$).

3. Results

3.1. H2 exhibits infectivity in Ifnar$^{-/-}$ mice

To establish small rodent animal models for the H2 strain, *Ifnar*$^{-/-}$ mice were infected with 10^7 RNA copies of the H2 strain through the intravenous (i.v) route (Fig. 1A). No clinical symptoms were observed during the observation period. Viral loads in serum and feces were detected, transient viremia was observed on day 7 post-infection, and the viral RNA was persistent until 21 days post-infection (Fig. 1B). Mock-treated mice showed no evidence of infection. In feces, viral RNA was detected on day 7 post-infection, persisted until 28 days, and was detected again on day 42 (Fig. 1C). All these data demonstrated that the H2 strain could infect *Ifnar*$^{-/-}$ mice and cause viremia and fecal shedding.

3.2. H2 strain replicates in the liver of Ifnar$^{-/-}$ mice

To evaluate whether H2 strain infection produced replication in the mice liver, *Ifnar*$^{-/-}$ mice were sacrificed at 42 days post-infection, and the viral load in the liver was detected. High levels of viral RNA were detected in the liver tissue of mice infected with the H2 strain, but not in that of the mock group mice (Fig. 2A). But no significant difference in ALT levels was observed between H2-infected and mock mice (Fig. 2B). Furthermore, the ISH assay also detected HAV-specific RNA in infected mice but no viral RNA in the liver of all mock-treated mice (Fig. 3). Similarly, the immunohistochemistry assay showed low HAV protein expressions in the hepatocyte of mice infected with the H2 strain, whereas no positive cells were detected in the liver of mock-treated mice (Fig. 3). All the results suggested that the H2 strain can replicate in the liver of *Ifnar*$^{-/-}$ mice.

ALT levels were not changed in H2-infected mice and mock mice (Fig. 2B). Nonetheless, histological analysis of the liver from *Ifnar*$^{-/-}$ mice showed focal infiltration of lymphocytes and neutrophils in the portal area of the liver tissue in H2-infected mice, but no focal necrosis was observed (Fig. 3). In contrast, mock-treated mice developed neither ALT content elevation nor hepatic inflammation. Thus, the H2 strain replicated in the liver of *Ifnar*$^{-/-}$ mice and led to slight pathological changes but could not induce the development of liver dysfunction.

3.3. H2 strain remains continuously infectious in the liver of Ifnar$^{-/-}$ mice

To confirm the infectivity and genetic stability of the H2 strain in the liver of *Ifnar*$^{-/-}$ mice, viruses isolated from mouse liver were inoculated into 2BS cells. The results showed that the HAV RNA can be detected in the cell cultures inoculated with the liver extract of infected mice and continuously increased (Fig. 4). Then, total RNA of the cell cultures was extracted, and the complete genome of the isolate was sequenced. There were only four nonsynonymous substitutions in the polyprotein gene

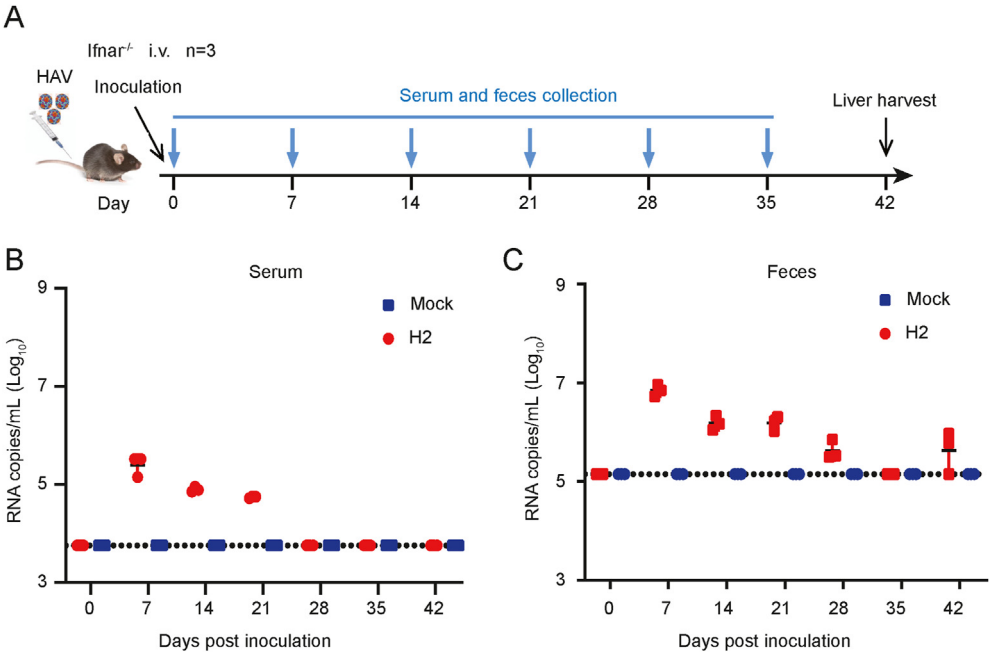

Fig. 1. H2 strain infection in *Ifnar*$^{-/-}$ mice. **A** Schematic diagram of inoculation and sampling in *Ifnar*$^{-/-}$ mice. **B** Serum HAV RNA in *Ifnar*$^{-/-}$ mice infected with 10^7 RNA copies of the H2 strain was quantified by real-time RT-qPCR. **C** Fecal HAV RNA in infected *Ifnar*$^{-/-}$ mice was quantified by real-time RT-qPCR. Dotted lines indicate the limits of detection.

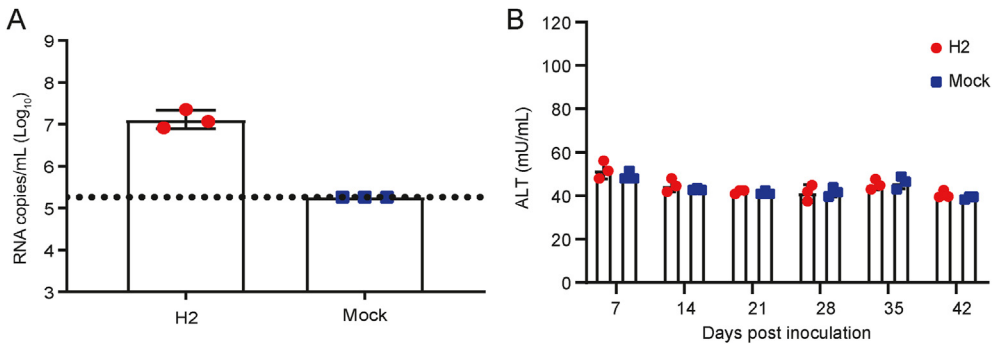

Fig. 2. Hepatic HAV RNA and ALT level in *Ifnar*$^{-/-}$ *mice* infected by H2 strain. **A** HAV RNA in the liver of *Ifnar*$^{-/-}$ mice at day 42 post-inoculation. Briefly, the liver was homogenized in DMEM followed by centrifugation at 8000×*g* for 10 min and detected by real-time RT-qPCR. Dotted lines indicate the limits of detection. **B** Serum ALT activity was measured using the alanine transaminase activity assay kit with Color Endpoint (Abcam, USA). *Ifnar*$^{-/-}$ mice were infected with 10^7 RNA copies of H2 strain and mice serum were collected at different time.

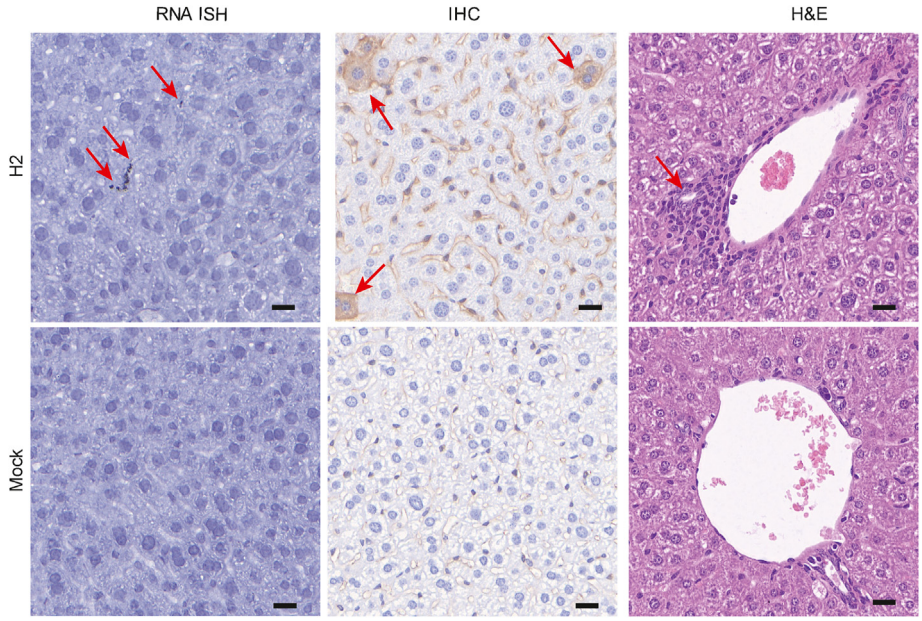

Fig. 3. H2 strain infection in the liver of *Ifnar*$^{-/-}$ *mice*. RNA ISH: ISH assay for HAV RNA detection in liver tissues. Red arrows show brown positive cells. IHC: Immunohistochemical staining of liver tissues with HAV-specific antibody. HAV protein is indicated in brown. Red arrows show brown positive cells. H&E: Histopathological assays of the mice liver. The red arrow shows inflammatory cell infiltration. Scale bars, 20 μm.

compared with the H2 strain (Table 1), resulting in 99.4% homology of the amino acid sequence. These data showed that the H2 strain continuously replicates in the liver and produces infectious progeny viruses.

3.4. H2 strain induces a special humoral immunity response in Ifnar$^{-/-}$ mice

Next, we investigated the immunogenicity profile of the H2 strain in *Ifnar*$^{-/-}$ mice, and HAV-specific IgG was detected in *Ifnar*$^{-/-}$ mice as early as day 7 post-infection (Fig. 5A); it reached the highest level (geometric mean titer, GMT = 51,200) on day 28, then gradually decreased until day 42, but still maintained a higher level (GMT = 26,667). As expected, no HAV-specific antibodies were detected in mock-treated mice. Importantly, virus neutralization assay showed that the mixture of HAV HM175/18f and serum of H2-infected mice produced only about 16 plaques, compared with 39 plaques in the NC group, indicating an effective virus inhibition of 57.6%, but virus neutralizing activities were not detected in the serum of mock mice (Fig. 5B), suggesting that the H2 can induce the production of neutralizing antibodies against HAV in *Ifnar*$^{-/-}$ mice. These data suggested that the H2 strain can induce robust humoral immune responses against HAV in *Ifnar*$^{-/-}$ mice.

4. Discussion

The small animal model is an effective platform to evaluate virulence and attenuated characteristics, vaccines design, and drugs development, although most research on HAV was conducted in nonhuman primates (Misumi et al., 2021). In this study, the infection and pathogenicity of the live attenuated HAV H2 strain were observed for the first time in *Ifnar*$^{-/-}$ mice.

On day 7 post-inoculation, virus RNA can be detected in serum, then continues to decline to the detection limit as time goes on. Because of the fact that HAV is an enterovirus transmitted by fecal-oral route, HAV can only appear a low virus load in the blood for a short time. A previous study showed that wild-type HAV infected *Ifnar*$^{-/-}$ mice exhibit only

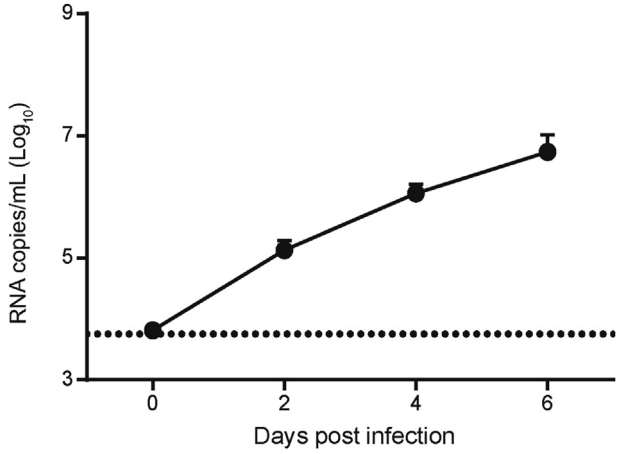

Fig. 4. Isolation of the virus from the liver of *Ifnar*$^{-/-}$ mice infected with the H2 stain. 2BS cells were inoculated with liver extracts from H2 strain-infected mice, and HAV RNA was detected in cell cultures at different time points. Dotted lines indicate the limits of detection.

Table 1
Nonsynonymous changes in the polyprotein sequence of the isolate from *Ifnar*$^{-/-}$ mice infected with the H2 strain.

Region	Amino acid position	Nucleotide change	Amino acid	
			H2 strain	The isolate
2A	893	CTG-CAG	Leu	Gln
	906	TTT-TGT	Phe	Cys
	916	AGC-GGT	Ser	Gly
2B	990	TTC-TCC	Phe	Ser

low-grade viremia (Hirai-Yuki et al., 2016a). In HAV-infected chimpanzees, HAV was cleared rapidly from the blood after 2–3 weeks of infection, and serum HAV RNA declined and was no longer detectable by 6–8 weeks (Lanford et al., 2011).

At present, the viral shedding characteristics of H2 strain *in vivo* have not been reported. Our study showed that the H2 strain can be detected in feces of infected *Ifnar*$^{-/-}$ mice on day 7 post-infection and persist for at least 42 days, but the virus was not isolated from the feces of infected mice when virus RNA copies in feces peaked on day 7 post-infection, which may be due to the lower levels of the virus in feces. In this study, we found that when the viral RNA load decreased to the limit of detection in feces, about 10^5 copies/g (Fig. 1C), the viral RNA load in the liver was about 10^7 copies/g on day 42 post-infection (Fig. 2A), suggesting that the viral RNA load in the liver remained high levels even after the fecal virus shedding had terminated. This phenomenon is consistent with HAV wild-type strain infection in *Ifnar*$^{-/-}$ mice (Hirai-Yuki et al., 2016a). Our data demonstrated the characteristic of continuous viral shedding of HAV in feces of *Ifnar*$^{-/-}$ mice infected with the H2 strain.

In our study, H2 strain infection did not cause obvious symptoms of liver damage in mice. There was no ALT elevation and only a slight inflammatory response in liver tissues, which is different from the pathogenicity of wild-type HAV in mice reported by Lemon et al. (Hirai-Yuki et al., 2016a). Lemon et al. found that the wild-type HAV infection resulted in increased ALT levels, hepatocyte apoptosis, and a secondary hepatic inflammatory response in *Ifnar*$^{-/-}$ mice. It seems that *Ifnar*$^{-/-}$ mice with 129Sv/Ev or C57BL/6 genetic backgrounds are different, which possibly shows different immunopathology following viral infection. In addition, liver injury is closely linked to the replicative capacity of the virus in the liver (Sun et al., 2021). Moreover, it has been reported that the 3ABC protein encoded by HAV has host-specific cleavage activity for MAVS and cannot degrade the MAVS protein of mice, thus leading to liver injury. The H2 strain acquired a large number of nucleotide mutations during passaging in cell cultures, some of which are located in the 3ABC segment (Huang et al., 1997). Further research is needed to identify whether these mutations are related to the failure of the H2 strain caused liver damage in mice.

HAV is capable of robustly infecting nonhuman primate animals, such as chimpanzees (Robertson et al., 1994), tamarins (Karayiannis et al., 2010), marmosets, rhesus monkeys (Chitambar et al., 2001), and owl monkeys firmly (Mao et al., 1988), and can establish hepatotropic infection with pathologic consequences similar to those in humans (Purcell and Emerson, 2001). However, there are many obstacles including ethical concerns, costs, and research policies on nonhuman primate models. Therefore, alternative models are rapidly being developed. H2 attenuated strain infection can induce the production of IgG and neutralizing antibodies in *Ifnar*$^{-/-}$ mice, and the dynamic changes of antibodies are similar to the immune response in humans infected with HAV (Lemon et al., 1997). Interestingly, we found that the production of high levels of IgG antibodies was induced in *Ifnar*$^{-/-}$ mice infected with the H2 strain as early as 7 days after infection. However, it has been reported that IgG antibodies can not be detected until 28 days after wild-type HAV strain infection in *Ifnar*$^{-/-}$ mice (Hirai-Yuki et al., 2016a). This difference may be related with the genetic background of *Ifnar*$^{-/-}$ mice. In our study, we used the *Ifnar*$^{-/-}$ mice based on 129Sv/Ev mice, while Hirai-Yuki et al. used the B6 mice deficient in type I IFN receptors. In addition, in our study, the polyprotein gene sequence of HAV isolated from the liver extracts of infected mice is almost identical to that of the H2 strain, demonstrating that the H2 strain has genetic stability in mouse

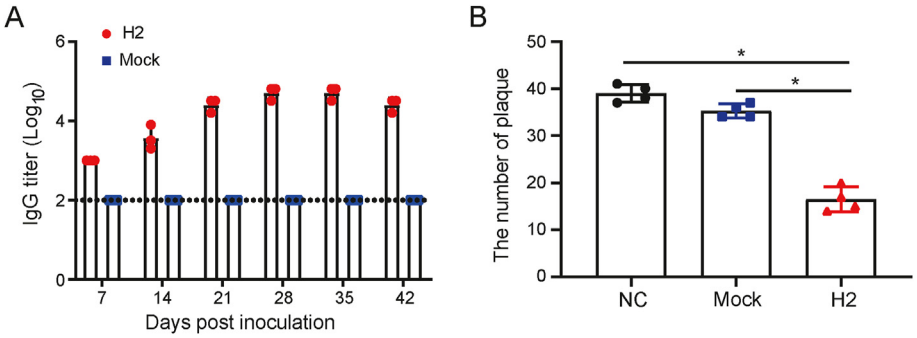

Fig. 5. Humoral immune responses in *Ifnar*$^{-/-}$ mice infected with the H2 strain. **A** HAV-specific IgG antibody titers of infected *Ifnar*$^{-/-}$ mice at different time points were determined by ELISA at different time points. Dotted lines indicate the limits of detection. **B** Virus neutralization assay. Wild type HAV (HM175/18f strain) was incubated with heat-inactivated serum of H2 infected *Ifnar*$^{-/-}$ mice or uninfected mock group or PBS, respectively, on day 42 post-inoculation (H2 or mock group) or PBS (negative control, NC group), and the mixture was used to infect BS-C-1 cells in 12-well plates to detect anti-HAV neutralizing antibodies. Data are shown as the mean ± SEM. Significance was calculated using nonparametric statistical analysis (*$P < 0.05$).

models. These characteristics are necessary for an effective and safe animal model for vaccine and drug evaluations.

5. Conclusions

In conclusion, this study describes the characteristics of *Ifnar*$^{-/-}$ mice infected with a live attenuated hepatitis A vaccine (H2 strain), including viremia, virus shedding, virus replication in liver tissue, and humoral immune responses. These data can provide useful information regarding the possible attenuating mechanisms of the H2 strain. This mouse model of H2 strain infection is expected as a safer animal model for screening vaccines and antiviral drugs against hepatitis A.

Data availability

All the data generated during the current study are included in the manuscript and/or the Supplementary data. Additional data related to this article may be requested from the corresponding authors.

Ethics statement

All procedures involving infectious viruses were conducted in Biosafety Level 2 laboratory (BSL-2) at Beijing Institute of Microbiology and Epidemiology and approved by the Animal Experiment Committee of Laboratory. Research involving *Ifnar*$^{-/-}$ mice was approved by and carried out in strict accordance with the guidelines of the Institutional Experimental Animal Welfare and Ethics Committee (IACUC-DWZX-2020-001).

Author contributions

Cheng-Feng Qin and Hui Zhao: formal analysis, investigation, supervision, writing – review & editing. Qing-Qing Ma and Hong-Jiang Wang: methodology, data curation, writing – original draft, writing – review & editing. Jian Li and Meng-Qi Li: methodology, visualization, data curation. Tian-Shu Cao, Xiao-Yan Wu, and Hong-Ying Qiu: methodology.

Conflict of interest

The authors declare no competing interests.

Acknowledgments

We thank Drs. Qiang-Ming Sun and Qiang Ding for sharing the HAV HM175/18f strain and their excellent technical support. We also thank Shi-Hui Sun for pathologic analysis. Cheng-Feng Qin was supported by the National Natural Science Fund for Distinguished Young Scholar (No. 81925025), the Innovative Research Group (No. 81621005) from the National Natural Science Foundation of China, and the Innovation Fund for Medical Sciences (No. 2019-I2M-5-049) from the Chinese Academy of Medical Sciences.

Appendix A. Supplementary data

Supplementary data to this article can be found online at https://doi.org/10.1016/j.virs.2022.07.009.

References

Bamford, D.H., Zuckerman, M., 2021. Encyclopedia of Virology, fouth ed. Elsevier Ltd., Amsterdam, pp. 362–372.

Britt, Hornei, R.K, Pierre, Moubayed, Werner, Frings, Verena, Gauss, Müller, Andreas, Dotzauer, 2001. Experimental hepatitis A virus infection in Guinea pigs. J. Med. Virol. 64, 402.

Chitambar, S.D., Joshi, M.S., Sreenivasan, M.A., Arankalle, V.A., 2001. Fecal shedding of hepatitis A virus in Indian patients with hepatitis A and in experimentally infected Rhesus monkey. Hepatol. Res. 19, 237–246.

Daniel, S., Pierre, V.N., 2019. The Immunological Basis for Immunization Series: Module 18: Hepatitis A. World Health Organization, pp. 12–13. http://apps.who.int/iris/handle/10665/326501.

Drexler, J.F., Corman, V.M., Lukashev, A.N., van den Brand, J.M., Gmyl, A.P., Brünink, S., Rasche, A., Seggewiß, N., Feng, H., Leijten, L.M., 2015. Evolutionary origins of hepatitis A virus in small mammals. Proc. Natl. Acad. Sci. USA 112, 15190–15195.

Guidotti, L.G., Chisari, Fv, Murray, J.M., Purcell, R.H., Wieland, S.F., 2019. Immunobiology and pathogenesis of viral hepatitis. Annu. Rev. Pathol. 1, 23–61.

Hirai-Yuki, A., Hensley, L., Mcgivern, D.R., González-López, O., Das, A., Hui, F., Lu, S., Wilson, J.E., Hu, F., Feng, Z., 2016a. MAVS-dependent host species range and pathogenicity of human hepatitis A virus. Science 353, 1541–1545.

Hirai-Yuki, A., Hensley, L., Whitmire, J.K., Lemon, S.M., 2016b. Biliary secretion of quasi-enveloped human hepatitis A virus. mBio 7, e01998, 01916.

Huang, X., Lian, Y., Wang, Q., 1997. Experimental in vivo passage of H2 strain of live attenuated vaccine of hepatitis A in common marmosets. Chin. J. Prev. Med. 31, 260.

Karayiannis, P., Jowett, T., Enticott, M., Moore, D., Thomas, H.C., 2010. Hepatitis A virus replication in tamarins and host immune response in relation to pathogenesis of liver cell damage. J. Med. Virol. 18, 261–276.

Lanford, R.E., Feng, Z., Chavez, D., Guerra, B., Brasky, K.M., Zhou, Y., Yamane, R., Perelson, A.S., Walker, C.M., Lemon, S.M., 2011. Acute hepatitis A virus infection is associated with a limited type I interferon response and persistence of intrahepatic viral RNA. Proc. Natl. Acad. Sci. U.S.A. 108, 11223–11228.

Lemon, S.M., Murphy, P.C., Provost, P.J., Ira, C., Davide, J.P., Schofield, T.L., Nalin, D.R., Lewis, J.A., 1997. Immunoprecipitation and virus neutralization assays demonstrate qualitative differences between protective antibody responses to inactivated hepatitis A vaccine and passive immunization with immune globulin. J. Infect. Dis. 9–19.

Li, S.H., Dong, H., Li, X.F., Xie, X., Zhao, H., Deng, Y.Q., Wang, X.Y., Ye, Q., Zhu, S.Y., Wang, H.J., Zhang, B., Leng, Q.B., Zuest, R., Qin, E.D., Qin, C.F., Shi, P.Y., 2013. Rational design of a flavivirus vaccine by abolishing viral RNA 2'-0 methylation. J. Virol. 87, 5812–5819.

Luo, J., Wang, X., Ma, F., Kang, G., Ding, Z., Ye, C., Pan, Y., Zhao, Y., Hong, S., Chen, J., 2019. Long-term immunogenicity and immune persistence of live attenuated and inactivated hepatitis a vaccines: a report on additional observations from a phase IV study - ScienceDirect. Clin. Microbiol. Infect. 25, 1422–1427.

Mao, J.S., Dong, D.X., Zhang, H.Y., Chen, N.L., Zhang, X.Y., Huang, H.Y., Xie, R.Y., Zhou, T.J., Wan, Z.J., Wang, Y.Z., 1989. Primary study of attenuated live hepatitis A vaccine (H2 strain) in humans. J. Infect. Dis. 621–624.

Mao, J.S., Xie, R.Y., Huang, H.Y., Chai, S.A., Dong, D.X., 1988. Studies in monkeys of attenuated hepatitis A variants. Singapore Bus. 31, 338–343.

Mao, J.S., Go, Y.Y., Huang, H.Y., Yu, P.H., Huang, B.Z., Ding, Z.S., Chen, N.L., Yu, J.H., Xie, R.Y., 1981. Susceptibility of monkeys to human hepatitis A virus. J. Infect. Dis. 55–60.

Misumi, I., Mitchell, J.E., Lund, M.M., Cullen, J.M., Lemon, S.M., Whitmire, J.K., 2021. T cells protect against hepatitis A virus infection and limit infection-induced liver injury. J. Hepatol. 75, 1323–1334.

Oluwafemi, B., Ashley, B., Angelo, D., Hochberg, N.S., Barnett, E.D., Ambra, N.L., Hilmir, A., Grobusch, M.P., Karin, L., Fernando, S., 2022. Acute hepatitis a in international Travelers: a GeoSentinel analysis, 2008–2020. J. Trav. Med. 29 taac013.

Purcell, R.H., Emerson, S.U., 2001. Animal models of hepatitis A and E. I. L. AR (Anticancer Res.) J. 42, 161–177.

Rao, S., Mao, J.S., Motlekar, S., Fangcheng, Z., Kadhe, G., 2016. A review of immunogenicity and tolerability of live attenuated Hepatitis A vaccine in children. Hum. Vaccine 23, 3160–3165.

Robertson, B.H., D'Hondt, E.H., Spelbring, J., Tian, H., Margolis, H.S., 1994. Effect of postexposure vaccination in a chimpanzee model of hepatitis A virus infection. J. Med. Virol. 43, 249–251.

Shah, N., Faridi, M., Mitra, M., Bavdekar, A., Jain, R., 2020. Review of long term immunogenicity and tolerability of live hepatitis A vaccine. Hum. Vaccines Immunother. 1–6.

Sun, L., Li, Y., Misumi, I., González-López, O., Hensley, L., Cullen, J.M., McGivern, D.R., Matsuda, M., Suzuki, R., Sen, G.C., Hirai-Yuki, A., Whitmire, J.K., Lemon, S.M., 2021. IRF3-mediated pathogenicity in a murine model of human hepatitis A. PLoS. Pathog. 17, e1009960.

Yin, S., Laurie, B.,K.N., Greta, K., Foster, M.A., Jan, D., Jiles, R.B., 2020. Susceptibility to hepatitis A virus infection in the United States, 2007-2016. Clin. Infect. Dis. 71, e571–e579.

Zhuang, F.C., Wang, X.Y., Chen, M.D., Jiang, L.M., Wu, J., Jiang, Q., Gong, Y.P., Qian, W., Xin, Y.J., Mao, J.S., 2012. Era of vaccination heralds a decline in incidence of hepatitis A in high-risk groups in China. Hepat. Mon 12, 100–105.